Biochemistry and Biophysics Reports 27 (2021) 101075

Contents lists available at ScienceDirect

Biochemistry and Biophysics Reports

journal homepage: www.elsevier.com/locate/bbrep

Cytoprotection of rat hepatocytes by desipramine in a model of simulated ischemia/reperfusion

Jun-Kyu Shin [a], Jae-Sung Kim [a,b,*]

[a] Department of Surgery, Washington University in St. Louis, St. Louis, MO, 63110, USA
[b] Department of Cell Biology & Physiology, Washington University in St. Louis, St. Louis, MO, 63110, USA

ARTICLE INFO

Keywords:
Desipramine
Autophagy
Liver
Ischemia and reperfusion injury

ABSTRACT

We investigated the cytoprotective effect of desipramine (DMI) during *in vitro* simulated ischemia/reperfusion (I/R) of rat hepatocytes. Primary hepatocytes isolated from male Sprague-Dawley rats were subjected to 4 h of anoxia at pH 6.2 followed by normoxia at pH 7.4 for 2 h to simulate ischemia and reperfusion, respectively. During simulated reperfusion, some hepatocytes were reoxygenated using media containing 5 μM DMI. Necrotic cell death and the onset of mitochondrial permeability transition (MPT) were assessed using fluorometry and confocal microscopy. Changes in autophagic flux and autophagy-related proteins (ATGs) were analyzed by immunoblotting. DMI was shown to substantially delay MPT onset and suppress I/R related cell damage. Mechanistically, DMI treatment during reperfusion increased the expression level of the microtubule-associated protein 1A/1B-light chain 3 (LC3) processing enzymes, ATG4B and ATG7. Genetic knockdown of ATG4B abolished the cytoprotective effect of DMI. Together, these results indicate that DMI is a unique agent which enhances LC3 processing in an ATG4B-dependent way.

1. Introduction

A temporary cessation and subsequent resumption of blood flow due to transient interruption of circulation during liver resection and transplantation can cause hepatic ischemia/reperfusion (I/R) injury. Mitochondrial dysfunction is a key cellular event which contributes to I/R injury [1]. After reperfusion, the integrity of mitochondrial inner membranes can become disrupted by the opening of permeability transition pores, nonspecific channels in the inner membrane, resulting in an uncontrolled influx of solutes up to 1500 Da in size into the mitochondrial matrix. Consequently, mitochondria depolarize and fail to generate adenosine triphosphate (ATP). This process is known as mitochondrial permeability transition (MPT). Despite the importance of MPT in mediating ischemic liver injury, current therapeutic strategies using the MPT blocker cyclosporin A have had limited impact in the clinical setting due to its narrow range of therapeutic efficacy [2] and its inhibition of calcineurin [3]. Furthermore, cyclosporin A-insensitive MPT can still occur when MPT induction increases [4].

Desipramine (DMI) is a Food and Drug Administration (FDA)-approved antidepressant first developed in 1962 [5] which has been reported to block the onset of MPT in the liver [6]. Numerous antidepressant drugs have been shown to affect autophagy in a variety of tissues [7]. Mitophagy is a form of selective autophagy which involves the degradation of surplus or dysfunctional mitochondria [8]. As defective mitophagy or insufficient rates of mitophagy result in the accumulation of dysfunctional mitochondria, the timely onset of mitophagy is critical to cellular survival. We have previously demonstrated that impaired mitophagy after I/R is a causative event contributing to MPT [8]. Accordingly, we hypothesized that significant levels of cytoprotection could be achieved during I/R injury by promoting autophagy and preventing the onset of MPT. As yet, it is unknown how DMI affects autophagy and I/R injury in the liver.

Here, we investigated the effects of DMI on an *in vitro* model of I/R injury using primary rat hepatocytes. Our results show that DMI stimulates autophagy in an ATG4B-dependent manner, suppressing the onset of MPT and reducing hepatocyte death after I/R injury.

2. Materials and methods

2.1. Isolation of primary rat hepatocytes

Animal experimental protocols were approved by the Animal Studies

* Corresponding author. Department of Surgery, Department of Cell Biology & Physiology, Washington University in St. Louis, St. Louis, MO, 63110, USA.
E-mail address: kjaesung@wustl.edu (J.-S. Kim).

https://doi.org/10.1016/j.bbrep.2021.101075
Received 6 April 2021; Received in revised form 29 June 2021; Accepted 8 July 2021

Committee at Washington University School of Medicine in St. Louis. Male Sprague Dawley rats (150–200 g; Charles River Laboratories, Wilmington, MA) were acclimated for at least 72 h prior to experimentation and standard rodent food and water was provided *ad libitum*. Primary hepatocytes were isolated using a two-step collagenase perfusion method, as previously described [8]. Greater than 90% cell viability, as assessed using the trypan blue exclusion assay, was required for all cells used in this study. Hepatocytes were cultured overnight in Dulbecco's Modified Eagle's Medium (DMEM) with 100 units/mL penicillin, 100 μg/mL streptomycin, 10% fetal bovine serum, 100 nM insulin, and 100 nM dexamethasone. For cell death assays, aliquots (0.5 mL) containing 2.0×10^5 hepatocytes were plated onto 24-well microtiter plates (Falcon, Lincoln Park, NJ). For confocal imaging, 2 mL of 2.0×10^5 cells were cultured on glass bottom 35-mm culture dishes. For immunoblot analysis, hepatocytes were plated on 35-mm culture dishes at a concentration of 10^6 cells/mL. All plates and dishes were coated with 0.1% Type I rat tail collagen. Hepatocytes were cultured in humidified 5% CO_2 and 95% air at 37 °C. Cells were washed three times with a fresh Krebs-Ringer-N-2-hydroxyethylpiperazine-N′-2-ethanesulfonic acid (HEPES) buffer (KRH) at pH 7.4 to remove unattached cells prior to ischemia. KRH buffer at pH 7.4 or pH 6.2 contained (in mM) 115 NaCl, 5 KCl, 2 $CaCl_2$, 1 KH_2PO_4, 1.2 $MgSO_4$, and 25 Na-HEPES. Target-specific gene delivery was performed using adenoviral vectors, as previously reported [8].

2.2. In vitro simulated I/R

To simulate tissue ischemia (referred to as ischemia hereafter), isolated hepatocytes were placed in anoxic KRH buffer at pH 6.2 in an anaerobic chamber (Coy Laboratory Products, Ann Arbor, MI) for 4 h. Anoxia was maintained at 37 °C under an atmosphere of 95% N_2–5% H_2 with a heated palladium catalyst to convert residual oxygen to water vapor. Oxygen tension in the chamber was less than 0.001 Torr, as routinely monitored by a gas analyzer (Model 10; Coy Laboratory Products). To simulate reoxygenation and recovery to normal intracellular pH which occurs during reperfusion, anoxic KRH buffer at pH 6.2 was replaced with aerobic KRH buffer at pH 7.4 (referred to as reperfusion hereafter) [8]. Reperfusion was continued for up to 2 h at 37 °C. Some hepatocytes were treated with 5 μM DMI for 20 min before reperfusion and continuously during reperfusion.

2.3. Cell death assay

Levels of necrotic cell death were determined at 5, 60, and 120 min post-reperfusion using propidium iodide (PI) fluorometry using a SpectraMax iD3 fluorescence reader (Molecular Devices, San Jose, CA), as described previously [8].

2.4. Confocal imaging of MPT onset

Hepatocytes cultured on glass bottom dishes were treated with a combination of 100 nM tetramethylrhodamine methylester (TMRM), 1 μM calcein-AM, and 3 μM PI to monitor mitochondrial membrane potential, MPT, and necrosis respectively, as previously described [8]. Confocal images were collected using an inverted Zeiss 880 laser scanning confocal microscope (Zeiss, Jena, Germany) equipped with a 63x N. A. 1.4 oil-immersion plan-apochromat lens. To visualize autophagosomes and mitophagosomes, hepatocytes infected with adenovirus encoding GFP-tagged LC3 (GFP-LC3) were labeled with TMRM [8]. Adenovirus expressing LacZ (Ad-LacZ) was used as a viral vector control. Confocal experiments were conducted at 37 °C.

2.5. Immunoblot analysis of autophagic flux and autophagy-related proteins (ATGs)

To measure autophagic flux, hepatocytes were treated with 20 μM chloroquine (CQ) for 20 min prior to reperfusion. Changes in LC3 expression were analyzed by immunoblotting [9]. Immunoblotting of ATG expression in the presence or absence of 5 μM DMI was conducted, as previously described [9]. The intensity of the immunoreactive bands was determined using TOTALLAB TL 120 software (Nonlinear Dynamics Ltd., Newcastle, UK).

2.6. Materials

The Antibodies used in this study were ATG3, ATG4B, ATG7, BECN1, BNIP3, Cathepsin D, LC3-I/II, mTOR, phospho-mTOR (Ser2448), AMPK, phospho-AMPK, phospho-ULK1 (Ser317), Rubicon, phospho-ULK1 (Ser757) (Cell Signaling Technology, Beverly, MA), LAMP-2 (Invitrogen, Carlsbad, CA), TFEB (Novus Biologicals, Littleton, CO), FIP200 (MilliporeSigma, St. Louis, MO), p62 (BD Biosciences, Franklin Lakes, NJ) and β-actin (Santa Cruz Biotechnology, Santa Cruz, CA). All other reagents used were of analytical grade and purchased from MilliporeSigma (St. Louis, MO).

2.7. Statistical analysis

The data were expressed as mean ± SE and obtained from at least 3 separate cell preparations. Differences between means were compared by the Student t-test using a level of significance of $p < 0.05$. Statistical analyses were performed using SigmaStat version 3 (Systat Software Inc, San Jose, CA).

3. Results

To simulate hepatic ischemia, rat hepatocytes were incubated in anaerobic, nutrient-deficient, and acidic KRH buffer (pH 6.2) at 37 °C. After 4 h of ischemic conditions, the anaerobic buffer was replaced with aerobic KRH buffer at pH 7.4. Similar to a previous report [8], hepatocyte death progressively increased after reperfusion (Fig. 1A). DMI at 5 μM significantly reduced cell death during 120 min of reperfusion, while a lower concentration (1 μM) did not. Hepatotoxicity was observed at 100 μM DMI.

Reperfusion of ischemic hepatocytes induces the opening of permeability transition pores, leading to uncoupling of oxidative phosphorylation and subsequent cell death [10]. Accordingly, we investigated whether DMI suppresses the onset of MPT after I/R (Fig. 1B). Calcein is a green fluorescent dye that is readily taken up into the cytosol and nucleus but is excluded by polarized mitochondria that electrophoretically accumulate TMRM. Consequently, functional mitochondria that have not undergone MPT appear as round, dark voids. Upon the development of MPT, mitochondria become depolarized, allowing calcein to redistribute from the cytosol into mitochondria and causing the disappearance of these calcein negative voids [8]. Along with calcein labelling of mitochondria that have undergone MPT, we used PI to label the nuclei of necrotic cells. After 4 h of ischemia, TMRM fluorescence was barely detectable due to anoxic depolarization of mitochondria. Mitochondria still excluded calcein under these conditions, indicating that MPT had not occurred. After 10 min of reperfusion, the mitochondria in 5 out of 6 cells repolarized while still excluding calcein. Following 20 min of reperfusion, one cell had undergone necrosis (yellow arrows) while another cell was dying (loss of TMRM). Widespread onset of MPT and subsequent necrosis ensued thereafter. After 60 min of reperfusion, 5 out of 6 cells had undergone necrosis. In sharp contrast, reperfusion with DMI markedly suppressed MPT onset and cell death (Fig. 1C). After 120 min of reperfusion, only one cell had become necrotic. Thus, these results demonstrate that DMI suppresses both the MPT and hepatocyte death after I/R.

Impaired autophagy is known to contribute to hepatic I/R injury [8]. Thus, we investigated whether DMI can act as a cytoprotective agent by blocking aberrant autophagy in reperfused hepatocytes. Autophagic flux was determined using CQ, a lysosomal inhibitor (Fig. 2A–C) [9]. The

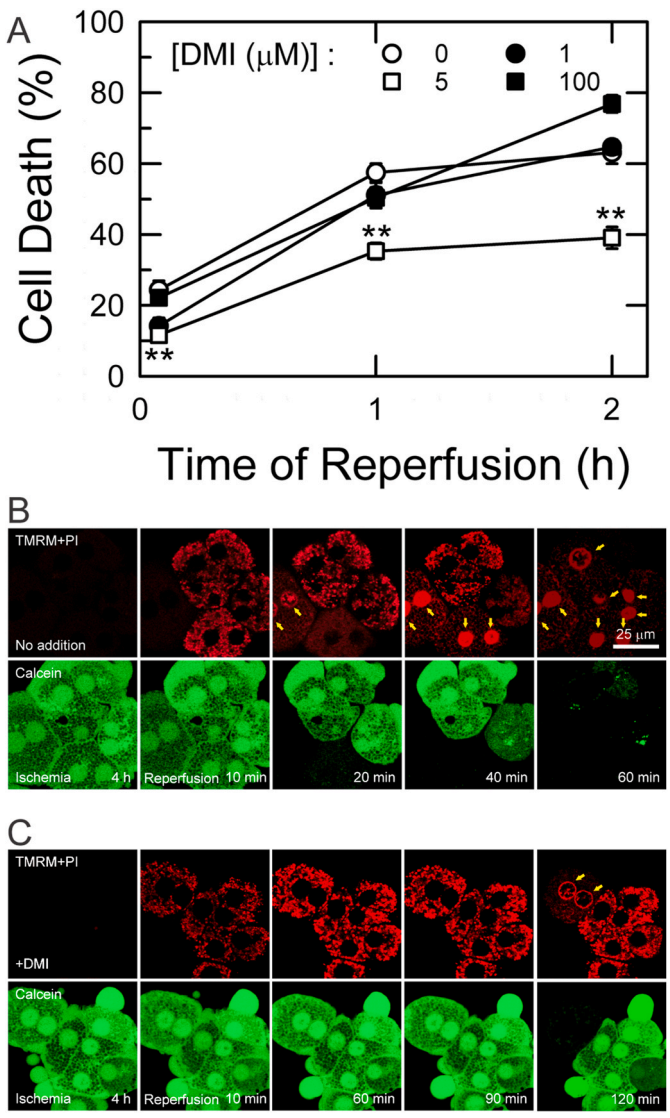

Fig. 1. Cytoprotection by DMI. (**A**) Cell death was determined after 5, 60, and 120 min of reperfusion following 4 h of ischemia (N = 8). **p < 0.01 vs no addition. (**B**) Confocal images of the onset of MPT, mitochondrial membrane potential, and necrosis during I/R were collected with 5 μM DMI. Arrows indicate a nuclear labeling of PI (cell death).

difference in LC3-II levels before and after CQ treatment indicates the net amount of autophagic cargo delivered to lysosomes. Both control and DMI-treated hepatocytes displayed similar levels of autophagic flux under normoxic conditions. After reperfusion, control cells displayed minimal autophagic flux, consistent with our previous report [8]. In stark contrast, cells reperfused with DMI had significantly greater autophagic flux after 2 h of reperfusion. Interestingly, autophagic flux in DMI-treated cells was lower than the control group after 1 h of reperfusion. Noticeably, a substantial reduction in levels of LC3-I, a non-lipidated form of LC3, was detected in the DMI-treated group after 20 min and 60 min of reperfusion, suggesting that DMI may be inducing alterations in LC3 processing. Changes in autophagic activity during I/R were also assessed via immunoblot analysis of p62 expression (Fig. 2D). DMI significantly decreased the expression of p62 after 1 h of reperfusion.

To further investigate DMI-mediated cytoprotection, confocal images were collected in GFP-LC3 and TMRM labeled hepatocytes to visualize autophagosomes and mitochondria, respectively (Fig. 3) [8]. When control cells were incubated in nutrient-rich DMEM, autophagosomes were barely visible (Fig. 3A and C), confirming minimal autophagic activity under nutrient-sufficient conditions. However, when cells were treated with DMI for 20 min, numerous autophagosomes were visible as green punctae. The number of autophagosomes per cell increased more than 6-fold after DMI treatment.

Starvation is a potent inducer of autophagy [2]. To examine the effects of DMI on autophagy under starvation conditions, cells were incubated for 2 h in nutrient-deficient KRH (Fig. 3B and C). As expected, the number of autophagosomes per cell markedly increased, from 2.2 to 25.0 per cell under these conditions, confirming robust induction of autophagy by starvation in these hepatocytes. DMI treatment further increased the number of autophagosomes to 86.0 per cell under starvation conditions. Noticeably, in the presence of DMI, numerous mitochondria were encircled by LC3-positive ring-like structures, indicative of the onset of mitophagy [8,11]. Moreover, the size of GFP-LC3 positive punctae and the number of positive ring-like structures were considerably greater in the DMI group as compared to controls. It is unlikely that the induction of mitophagy by DMI occurs as a result of altered mitochondrial membrane potential, as similar TMRM intensity levels are observed between treated and control cells. Together, these data demonstrate that DMI enhances mitophagy in hepatocytes.

Decreased LC3-I levels after DMI treatment (Fig. 2) prompted us to hypothesize that DMI augments LC3 processing, particularly the molecular step involving the conversion and recycling of LC3-II. LC3 processing is mediated by at least 3 different ATGs: ATG3, ATG4B, and ATG7 [12,13]. Immunoblot analysis revealed that DMI significantly increased ATG4B and ATG7 expression after 20 and 120 min of reperfusion (Fig. 4A and B). Although we observed an increasing trend in ATG3 levels, no statistical significant difference was achieved. We also analyzed the expression of other autophagy-related proteins involved in different stages of autophagy: (1) signaling and initiation (mTOR, AMPK, RUBICON, BNIP3, ULK1, and FIP200), (2) sequestration and maturation (BECN1 and ATG12-5), and (3) degradation (LAMP2 and cathepsin D) (Fig. 4B and C). Among these, only FIP200 levels were significantly increased by DMI treatment.

To investigate the underlying molecular mechanisms of DMI-mediated cytoprotection, we knocked down the expression of ATG4B in hepatocytes using an adenoviral vector expressing ATG4B short hairpin RNA (Ad-shATG4B) (Fig. 4D) [8]. Overnight incubation with different concentrations of adenovirus showed that a multiplicity of infection (MOI) of 30 reduced ATG4B expression by 65%. Higher viral concentrations did not enhance knockdown efficacy. The effect of Ad-shATG4B on cell death after I/R, with and without DMI, was examined with an MOI of 30. Hepatocytes treated with Ad-LacZ (viral control) developed time-dependent necrosis after reperfusion. As before, DMI significantly suppressed necrosis in control cells. However, knockdown of ATG4B expression abolished this suppression of necrosis. ATG4B knockdown alone slightly increased cell death only during the early phase of reperfusion. Taken together, these results suggest that ATG4B is a key component in DMI-mediated protection against I/R injury.

4. Discussion

Here we demonstrate that the FDA-approved drug DMI prevents the onset of MPT and promotes hepatocyte viability in an ATG4B-dependent manner after simulated I/R. Consistent with previous reports [8,9], our study confirmed the importance of mitochondria and autophagy in hepatic I/R injury (Fig. 1). DMI-mediated cytoprotection resulted from its autophagy inducing effect, as DMI was shown to enhance (1) autophagic flux after I/R (Fig. 2), and (2) the formation of autophagosomes and the onset of mitophagy under both nutrient-sufficient and -deficient conditions (Fig. 3). Mechanistically, ATG4B may play an integral role in DMI-mediated protection against I/R injury. We demonstrated that DMI increased the expression of ATG4B (Fig. 4A and B) and knockdown of ATG4B using targeted shRNA removed DMI's cytoprotective effect

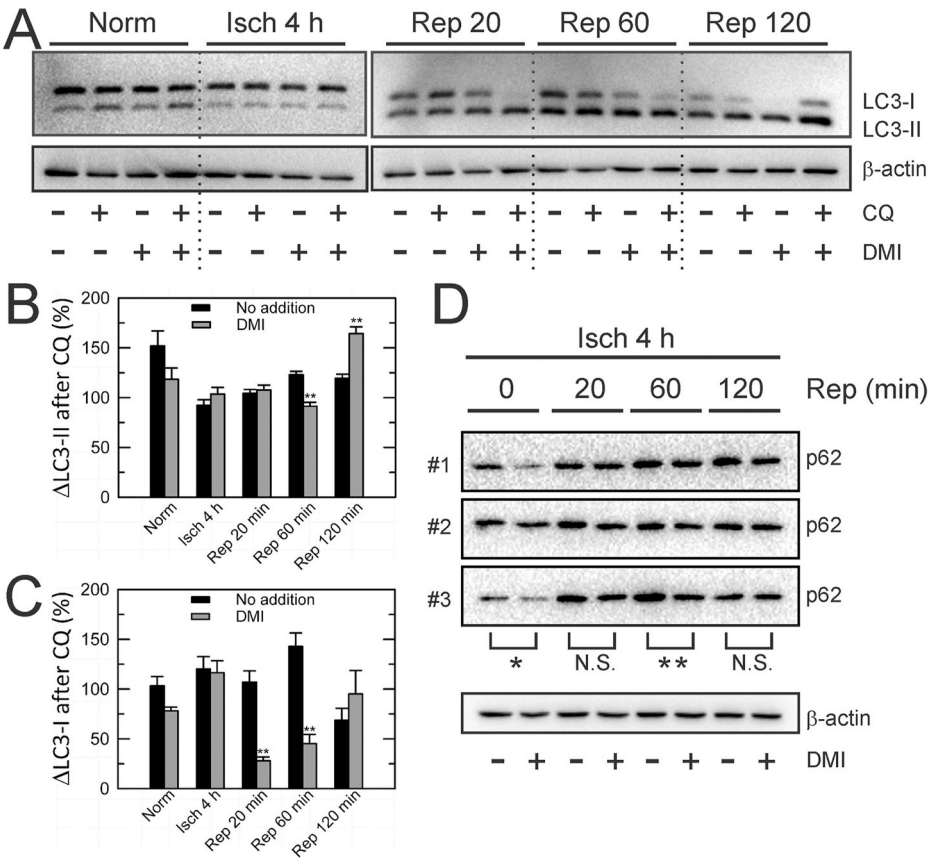

Fig. 2. Increased autophagic flux by DMI. (A) Autophagic flux in the presence or absence of 5 μM DMI was measured by immunoblotting LC3-II with 20 μM CQ (N = 4). Graphs represent the percent increase in (**B**) LC3-II and (**C**) LC3-I at given times after the addition of CQ. **p < 0.01 vs no addition. (**D**) Autophagic activity during I/R was also assessed by immunoblotting p62 from hepatocytes with and without DMI treatment (N = 3). The changes in LC3-I/II or p62 were normalized to β-actin before quantification. *p < 0.05 and **p < 0.01; N.S.: not significant.

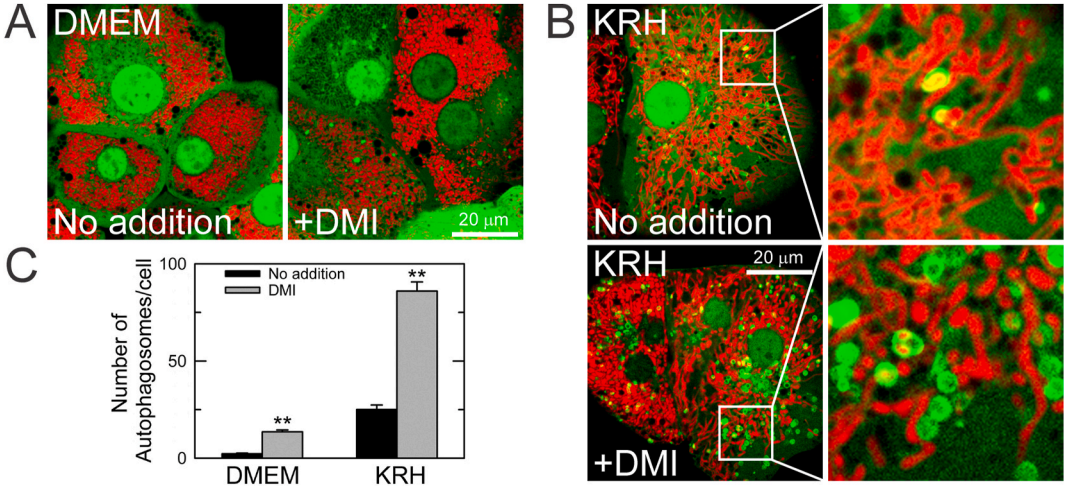

Fig. 3. Enhanced formation of autophagosomes by DMI treatment. Confocal images of GFP-LC3 (green) and TMRM (red) with and without 5 μM DMI treatment were collected in (**A**) nutrient-rich DMEM and (**B**) nutrient-deficient KRH. The right panels in the KRH group represent enlarged images of the square inset. (**C**) The number of autophagosomes per hepatocyte was counted from 39 different fields of view. **p < 0.01 vs no addition. (For interpretation of the references to colour in this figure legend, the reader is referred to the Web version of this article.)

(Fig. 4D).

A key finding in the present study is the modulatory effect of DMI on ATG4B expression levels. ATG4B is a cysteine protease with a catalytic triad of Cys74, Asp278, and His280 residues [14]. LC3 is processed by three distinct steps, (1) proteolytic cleavage of pro-LC3 into LC3-I by ATG4B, (2) generation of LC3-II through the lipidation of LC3-I with phosphatidylethanolamine (PE) by ATG3 and ATG7, and (3) removal of the PE moiety from LC3-II and recycling of LC3-I by ATG4B [14–16]. We found that DMI treatment caused a significant increase in both ATG4B and ATG7 levels. Moreover, immunoblot analysis of LC3-I/II revealed unique changes in LC3-I levels induced by DMI during I/R. LC3-I levels remained unaltered during 4 h of ischemia in both groups, but there were noticeable reductions in LC3-I after reperfusion. While LC3-1 levels in control cells were considerably reduced after 120 min of reperfusion, DMI-treated cells showed a significant loss of LC3-I from 20 min after commencement of reperfusion. After 120 min, LC3-I expression was barely detectable in DMI-treated cells. When CQ was added to block the degradation of cargo molecules in autophagosomes, reductions in LC3-I

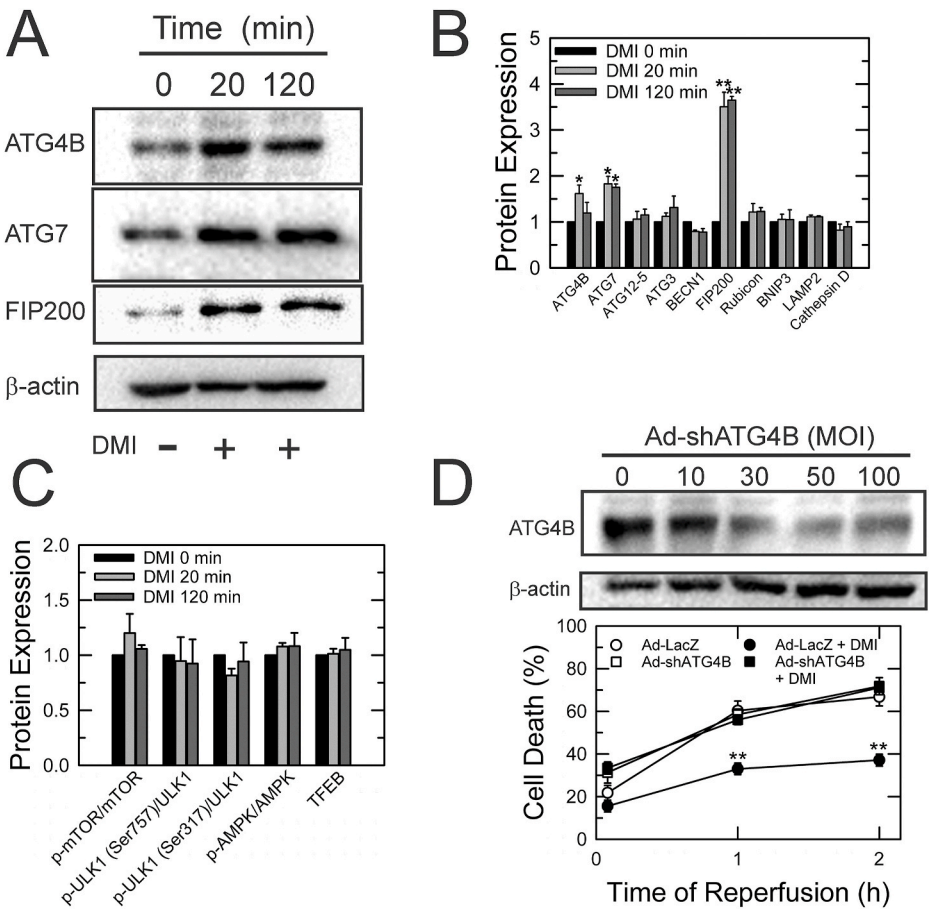

Fig. 4. The role of ATG4B in DMI-mediated cytoprotection. (**A**) Changes in autophagy protein levels were determined by immunoblot analysis after normoxically incubating hepatocytes with 5 μM DMI for 0, 20, and 120 min (N = 3). (**B & C**) Graphs represent fold-increases in autophagy protein levels relative to baseline, 0 min after DMI treatment. *p < 0.05 and **p < 0.01 vs DMI 0 min. (**D**) Cell death after I/R was determined after adenoviral knockdown of ATG4B. **p < 0.01 vs Ad-LacZ.

expression were also observed in DMI-treated cells at 20 and 60 min after commencement of reperfusion. Intriguingly, CQ treatment significantly increased LC3-I levels at 120 min. The reduction in LC3-I levels could occur (1) if PE mediated lipidation of LC3-I to LC3-II outpaces de novo synthesis of LC3, or (2) if LC3-I is recycled back to LC3-II by ATG4B [17]. The former scenario is less likely as the changes in LC3-II levels from 60 min to 120 min of reperfusion were minimal in both groups. In addition, ischemic hepatocytes lose 97% of ATP during 60 min of reperfusion [18]. Hence, a highly ATP-consuming de novo synthesis of LC3 is energetically unfavorable in reperfused cells. The idea that DMI treatment induces enhanced recycling of LC3-I was also supported by our observation that the total LC3 levels during 60 min of reperfusion, as estimated by the sum of LC3-I and LC3-II on immunoblots, remained similar before and after the addition of CQ.

Another noteworthy finding is that CQ treatment at 120 min of reperfusion markedly elevated levels of total LC3 in DMI-treated cells, but not in control cells, implying that DMI-treated hepatocytes may stimulate de novo synthesis of LC3 in the later stage of reperfusion. As the synthesis of new autophagy proteins is an ATP-dependent process, recycling of LC3-I/II may allow hepatocytes to reserve cellular energy that could be used for other vital ATP-consuming reactions. Reperfused hepatocytes recover only 30–40% of basal ATP, even with treatment with cyclosporin A, an MPT blocker which prevents hepatocyte death after I/R [18]. Thus, hepatocytes are likely to benefit energetically from LC3 recycling.

The present study has revealed a new function of DMI; regulation of LC3 processing in an ATG4B-dependent manner. Although DMI was initially developed for the treatment of depression, it is clear that this tricyclic agent is multi-functional. Besides its blockage of the reuptake of norepinephrine and serotonin in the brain [5], DMI has been known to inhibit acid sphingomyelinase (aSMase) [19] and acid ceramidase [20]. In mouse livers, it has been proposed that imipramine, a metabolic precursor of DMI [21], blocks aSMase and attenuates I/R injury [22]. However, imipramine binding may not be aSMase-specific and could elicit many off-target effects. Indeed, impaired autophagy was observed in hepatocytes isolated from aSMase knockout mice [23]. In non-hepatic cells, genetic ablation of aSMase suppressed the formation of autophagosomes [24]. Unlike imipramine, DMI stimulates autophagy in glioma cells [25]. As aSMase is predominantly localized to lysosomes [26] and lysosomal accumulation of DMI does not occur at a significant rate after transient exposure [27], DMI-mediated stimulation of autophagy is likely to be independent of aSMase.

Four different isoforms of ATG4 exist in mammalian cells, all of which are able to process LC3/GABA type A receptor-associated protein (GABARAP) family [28]. Among them, ATG4B is the major isoform and can cleave all seven members of the LC3/GABARAP family [29]. ATG4A is known to preferentially process GABARAP at a slower rate, while the processing of LC3/GABARAP family by either ATG4C or ATG4D was nominal [29]. Although we did not test the effects of other isoforms, their involvement in DMI-mediated LC3 processing is unlikely.

DMI also significantly increased the expression of FIP200, an initiator of autophagy [30], indicating that DMI's autophagy inducing effect may occur during the initiation stage of autophagy. However, neither Ser317 nor Ser757 of ULK1 was phosphorylated after DMI treatment. Phosphorylation of ULK1 at Ser317 by AMPK promotes autophagy, whereas mTOR-dependent phosphorylation of ULK1 at Ser757 prevents

autophagy [31]. In addition, we could not observe evidence for the activation of either AMPK or mTOR by DMI. Thus, it is likely that the mechanism of action of DMI-mediated cytoprotection in reperfused hepatocytes occurs through alterations to LC3 processing rather than through alterations to autophagy initiation. Future studies are warranted to elucidate how FIP200 affects LC3 processing.

Despite the novel findings described herein, our study is not without limitations. Firstly, *in vivo* I/R experiments are needed to validate the *in vitro* primary hepatocyte data into more clinically relevant models. Secondly, autophagic flux over the course of I/R as measured using p62 was not identical to that observed with LC3-II. Importantly, unlike LC3-II, cellular p62 can exist either in a soluble form or in detergent-resistant aggregates [32]. Moreover, it has been documented that p62 expression is cell type-specific and does not always inversely correlate with autophagic activity [33].

In conclusion, we have shown that DMI promotes autophagy by enhancing in ATG4B-mediated LC3 processing, thereby suppressing the onset of MPT and protecting hepatocytes from necrotic death after I/R. DMI as an autophagy-regulating agent represents a novel potential therapeutic approach to protecting hepatocytes and improving hepatic function after I/R.

Declaration of competing interest

Declare No Conflict of Interest by J-K Shin and J-S Kim.

Acknowledgements

This work was supported by the National Institutes of Health (R01 DK079879); Mid-America Transplant Foundation (07201903); and Foundation for Barnes-Jewish Hospital (4776, 5153).

The manuscript was edited by Dr. Paul S. Cassidy, the Scientific Editor of the Institute of Clinical and Translational Sciences at Washington University, which is supported by an NIH Clinical and Translational Science Award (UL1 TR002345).

Appendix A. Supplementary data

Supplementary data to this article can be found online at https://doi.org/10.1016/j.bbrep.2021.101075.

References

[1] J.S. Kim, L. He, J.J. Lemasters, Mitochondrial permeability transition: a common pathway to necrosis and apoptosis, Biochem. Biophys. Res. Commun. 304 (2003) 463–470, https://doi.org/10.1016/s0006-291x(03)00618-1.

[2] T. Qian, A.L. Nieminen, B. Herman, J.J. Lemasters, et al., Mitochondrial permeability transition in pH-dependent reperfusion injury to rat hepatocytes, Am. J. Physiol. 273 (1997) C1783–C1792, https://doi.org/10.1152/ajpcell.1997.273.6.C1783.

[3] S.L. Schreiber, G.R. Crabtree, The mechanism of action of cyclosporin A and FK506, Immunol. Today 13 (1992) 136–142, https://doi.org/10.1016/0167-5699(92)90111-J.

[4] L. He, J.J. Lemasters, Regulated and unregulated mitochondrial permeability transition pores: a new paradigm of pore structure and function? FEBS Lett. 512 (2002) 1–7, https://doi.org/10.1016/s0014-5793(01)03314-2.

[5] J. Andersen, A.S. Kristensen, B. Bang-Andersen, et al., Recent advances in the understanding of the interaction of antidepressant drugs with serotonin and norepinephrine transporters, Chem. Commun. 7 (2009) 3677–3692, https://doi.org/10.1039/b903035m.

[6] L. Luo, Y. Xie, A. Wang, et al., Desipramine ameliorates Cr(VI)-induced hepatocellular apoptosis via the inhibition of ceramide channel formation and mitochondrial PTP opening, Cell. Physiol. Biochem. 34 (2014) 2128–2136, https://doi.org/10.1159/000369657.

[7] N.C. Gassen, T. Rein, Is there a role of autophagy in depression and antidepressant action? Front. Psychiatr. 10 (2019) 337, https://doi.org/10.3389/fpsyt.2019.00337.

[8] J.S. Kim, T. Nitta, D. Mohuczy, et al., Impaired autophagy: a mechanism of mitochondrial dysfunction in anoxic rat hepatocytes, Hepatology 47 (2008) 1725–1736, https://doi.org/10.1002/hep.22187.

[9] T.G. Biel, S. Lee, J.A. Flores-Toro, et al., Sirtuin 1 suppresses mitochondrial dysfunction of ischemic mouse livers in a mitofusin 2-dependent manner, Cell Death Differ. 23 (2016) 279–290, https://doi.org/10.1038/cdd.2015.96.

[10] J.S. Kim, T. Qian, J.J. Lemasters, Mitochondrial permeability transition in the switch from necrotic to apoptotic cell death in ischemic rat hepatocytes, Gastroenterology 124 (2003) 494–503, https://doi.org/10.1053/gast.2003.50059.

[11] J.H. Wang, I.S. Ahn, T.D. Fischer, et al., Autophagy suppresses age-dependent ischemia and reperfusion injury in livers of mice, Gastroenterology 141 (2011) 2188–2199, https://doi.org/10.1053/j.gastro.2011.08.005.

[12] N. Fujita, M. Hayashi-Nishino, H. Fukumoto, et al., An Atg4B mutant hampers the lipidation of LC3 paralogues and causes defects in autophagosome closure, Mol. Biol. Cell 19 (2008) 4651–4659, https://doi.org/10.1091/mbc.e08-03-0312.

[13] A. Agrotis, R. Ketteler, On ATG4B as drug target for treatment of solid tumours-the knowns and the unknowns, Cells 9 (2019) 53, https://doi.org/10.3390/cells9010053.

[14] T. Kumanomidou, T. Mizushima, M. Komatsu, et al., The crystal structure of human Atg4b, a processing and de-conjugating enzyme for autophagosome-forming modifiers, J. Mol. Biol. 355 (2006) 612–618, https://doi.org/10.1016/j.jmb.2005.11.018.

[15] Y. Kabeya, N. Mizushima, T. Ueno, et al., LC3, a mammalian homologue of yeast Apg8p, is localized in autophagosome membranes after processing, EMBO J. 19 (2000) 5720–5728, https://doi.org/10.1093/emboj/19.21.5720.

[16] I. Tanida, Y.S. Sou, J. Ezaki, et al., HsAtg4B/HsApg4B/autophagin-1 cleaves the carboxyl termini of three human Atg8 homologues and delipidates microtubule-associated protein light chain 3- and GABAA receptor-associated protein-phospholipid conjugates, J. Biol. Chem. 279 (2004) 36268–36276, https://doi.org/10.1074/jbc.M401461200.

[17] R.A. Gottlieb, A.M. Andres, J. Sin, et al., Untangling autophagy measurements: all fluxed up, Circ. Res. 116 (2015) 504–514, https://doi.org/10.1161/CIRCRESAHA.116.303787.

[18] T. Qian, A.L. Nieminen, B. Herman, et al., Mitochondrial permeability transition in pH-dependent reperfusion injury to rat hepatocytes, Am. J. Physiol. 273 (1997) 1783–1792, https://doi.org/10.1152/ajpcell.1997.273.6.C1783.

[19] S. Albouz, J.J. Hauw, Y. Berwald-Netter, et al., Tricyclic antidepressants induce sphingomyelinase deficiency in fibroblast and neuroblastoma cell cultures, Biomedicine 35 (1981) 218–220.

[20] S. Elojeimy, D.H. Holman, X. Liu, et al., New insights on the use of desipramine as an inhibitor for acid ceramidase, FEBS Lett. 580 (2006) 4751–4756, https://doi.org/10.1016/j.febslet.2006.07.071.

[21] B. Brodie, P. Dick, P. Kielholz, et al., Preliminary pharmacological and clinical results with desmethylimipramine (DMI) G 35020, a metabolite of imipramine, Psychopharmacologia 2 (1961) 467–474, https://doi.org/10.1007/BF00407446.

[22] L. Llacuna 1, M. Marí, C. Garcia-Ruiz, et al., Critical role of acidic sphingomyelinase in murine hepatic ischemia-reperfusion injury, Hepatology 44 (2006) 561–572, https://doi.org/10.1002/hep.21285.

[23] R. Fucho, L. Martinez, A. Baulies, et al., ASMase regulates autophagy and lysosomal membrane permeabilization and its inhibition prevents early stage nonalcoholic steatohepatitis, J. Hepatol. 61 (2014) 1126–1134, https://doi.org/10.1016/j.jhep.2014.06.009.

[24] M. Taniguchi, K. Kitatani, T. Kondo, et al., Regulation of autophagy and its associated cell death by "sphingolipid rheostat": reciprocal role of ceramide and sphingosine 1-phosphate in the mammalian target of rapamycin pathway, J. Biol. Chem. 287 (2012) 39898–39910, https://doi.org/10.1074/jbc.M112.416552.

[25] J. Ma, L.N. Hou, Z.X. Rong, et al., Antidepressant desipramine leads to C6 glioma cell autophagy: implication for the adjuvant therapy of cancer, Anticanc. Agents Med. Chem. 13 (2013) 254–260, https://doi.org/10.2174/1871520611313020011.

[26] S. Fowler, Lysosomal localization of sphingomyelinase in rat liver, Biochim. Biophys. Acta 191 (1969) 481–484, https://doi.org/10.1016/0005-2744(69)90271-x.

[27] R. Fauster, U. Honegger, U. Wiesmann, Inhibition of phospholipid degradation and changes of the phospholipid-pattern by desipramine in cultured human fibroblasts, Biochem. Pharmacol. 32 (1983) 1737–1744, https://doi.org/10.1016/0006-2952(83)90119-3.

[28] K.J. Kauffman, S. Yu, J. Jin, et al., Delipidation of mammalian Atg8-family proteins by each of the four ATG4 proteases, Autophagy 14 (2018) 992–1010, https://doi.org/10.1080/15548627.2018.1437341.

[29] M. Li, Y. Hou, J. Wang, et al., Kinetics comparisons of mammalian Atg4 homologues indicate selective preferences toward diverse Atg8 substrates, J. Biol. Chem. 286 (2011) 7327–7338, https://doi.org/10.1074/jbc.M110.199059.

[30] T. Hara, A. Takamura, C. Kishi, et al., FIP200, a ULK-interacting protein, is required for autophagosome formation in mammalian cells, J. Cell Biol. 181 (2008) 497–510, https://doi.org/10.1083/jcb.200712064.

[31] J. Kim, M. Kundu, B. Viollet, et al., AMPK and mTOR regulate autophagy through direct phosphorylation of Ulk1, Nat. Cell Biol. 13 (2011) 132–141, https://doi.org/10.1038/ncb2152.

[32] R.A. Gottlieb, A.M. Andres, J. Sin, et al., Untangling autophagy measurements: all fluxed up, Circ. Res. 116 (2015) 504–514, https://doi.org/10.1161/CIRCRESAHA.116.303787.

[33] M.H. Sahani, E. Itakura, N. Mizushima, Expression of the autophagy substrate SQSTM1/p62 is restored during prolonged starvation depending on transcriptional upregulation and autophagy-derived amino acids, Autophagy 10 (2014) 431–441, https://doi.org/10.4161/auto.27344.